

¹ PeriDEM – High-fidelity modeling of granular media consisting of deformable complex-shaped particles

³ **Prashant Kumar Jha**  ¹

⁴ ¹ Department of Mechanical Engineering, South Dakota School of Mines and Technology, Rapid City,
⁵ SD 57701, USA

DOI: [10.xxxxxx/draft](https://doi.org/10.xxxxxx/draft)

Software

- ⁶ [Review](#) 
- ⁷ [Repository](#) 
- ⁸ [Archive](#) 

Editor: [Open Journals](#) 

Reviewers:

- ⁹ [@openjournals](#)

Submitted: 01 January 1970

Published: unpublished

License

Authors of papers retain copyright and release the work under a ¹⁷ Creative Commons Attribution 4.0 International License ([CC BY 4.0](#))¹⁸

Summary

⁷ Accurate simulation of granular materials under extreme mechanical conditions, such as crushing, fracture, and large deformation, remains a significant challenge in geotechnical, manufacturing, and mining applications. Classical discrete element method (DEM) models typically treat particles as rigid or nearly rigid bodies, limiting their ability to capture internal deformation and fracture. The PeriDEM library, first introduced in ([Jha et al., 2021](#)), addresses this limitation by modeling particles as deformable solids using peridynamics, a nonlocal continuum theory that naturally accommodates fracture and significant deformation. Inter-particle contact is handled using DEM-inspired local laws, enabling realistic interaction between complex-shaped particles.

¹⁶ Implemented in C++, PeriDEM is designed for extensibility and ease of deployment. It relies on a minimal set of external libraries, supports multithreaded execution, and includes demonstration examples involving compaction, fracture, and rotational dynamics. The framework facilitates granular-scale simulations, supports the development of constitutive models, and serves as a foundation for multi-fidelity coupling in real-world applications.

Statement of Need

²² Granular materials play a central role in many engineered systems, but modeling their behavior under high loading, deformation, and fragmentation remains an open problem. Popular open-source DEM codes such as YADE ([Smilauer et al., 2021](#)), BlazeDEM ([Govender et al., 2016](#)), Chrono DEM-Engine ([Zhang et al., 2024](#)), and LAMMPS ([Thompson et al., 2022](#)) are widely used but typically treat particles as rigid, limiting their accuracy in scenarios involving internal deformation and breakage. A recent review by Dosta et al. ([Dosta et al., 2024](#)) compares several DEM libraries. Meanwhile, peridynamics-based codes such as Peridigm ([Littlewood et al., 2024](#)) and NLMech ([Jha & Diehl, 2021](#)) are aimed at simulating deformation and fracture within a single structure, with limited support for multi-structure simulations.

³¹ PeriDEM fills this gap by integrating state-based peridynamics for intra-particle deformation with DEM-style contact laws for particle interactions. This hybrid approach enables direct simulation of particle fragmentation, stress redistribution, and dynamic failure propagation—capabilities essential for modeling granular compaction, attrition, and crushing.

³⁵ Recent multiscale approaches, including DEM-continuum and DEM-level-set coupling methods ([Harmon et al., 2021](#)), aim to bridge scales but often rely on homogenization assumptions. Sand crushing in geotechnical systems, for example, has been modeled using micro-CT-informed FEM or phenomenological laws ([Chen et al., 2023](#)). PeriDEM offers a particle-resolved alternative that allows bottom-up investigation of granular failure and shape evolution, especially in systems where fragment dynamics are critical.

⁴¹ Background

⁴² The PeriDEM model was introduced in ([Jha et al., 2021](#)), demonstrating its ability to model
⁴³ inter-particle contact and intra-particle fracture for complex-shaped particles. It is briefly
⁴⁴ described next.

⁴⁵ Brief Introduction to PeriDEM Model

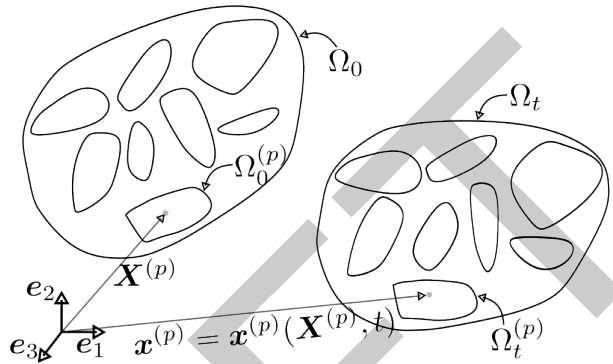


Figure 1: Motion of particle system.

⁴⁶ Consider a fixed frame of reference and $\{e_i\}_{i=1}^d$ are orthonormal bases. Consider a collection
⁴⁷ of N_P particles $\Omega_0^{(p)}$, $1 \leq p \leq N_P$, where $\Omega_0^{(p)} \subset \mathbb{R}^d$ with $d = 2, 3$ represents the initial
⁴⁸ configuration of particle p . Suppose $\Omega_0 \supset \cup_{p=1}^{N_P} \Omega_0^{(p)}$ is the domain containing all particles; see
⁴⁹ [Figure 1](#). The particles in Ω_0 are dynamically evolving due to external boundary conditions and
⁵⁰ internal interactions; let $\Omega_t^{(p)}$ denote the configuration of particle p at time $t \in (0, t_F]$, and
⁵¹ $\Omega_t \supset \cup_{p=1}^{N_P} \Omega_t^{(p)}$ domain containing all particles at that time. The motion $x^{(p)} = x^{(p)}(\mathbf{X}^{(p)}, t)$
⁵² takes point $\mathbf{X}^{(p)} \in \Omega_0^{(p)}$ to $x^{(p)} \in \Omega_t^{(p)}$, and collectively, the motion is given by $\mathbf{x} = \mathbf{x}(\mathbf{X}, t) \in$
⁵³ Ω_t for $\mathbf{X} \in \Omega_0$. We assume the media is dry and not influenced by factors other than
⁵⁴ mechanical loading (e.g., moisture and temperature are not considered). The configuration of
⁵⁵ particles in Ω_t at time t depends on various factors, such as material and geometrical properties,
⁵⁶ contact mechanism, and external loading. Essentially, there are two types of interactions
⁵⁷ present in the media:

- ⁵⁸ \blacksquare *Intra-particle interaction* that models the deformation and internal forces in the particle
⁵⁹ and
- ⁶⁰ \blacksquare *Inter-particle interaction* that accounts for the contact between particles and the boundary
⁶¹ of the domain in which the particles are contained.

⁶² In DEM, the first interaction is ignored, assuming that particle deformation is insignificant
⁶³ compared to inter-particle interactions. On the other hand, PeriDEM accounts for both
⁶⁴ interactions.

⁶⁵ The balance of linear momentum for particle p , $1 \leq p \leq N_P$, takes the form:

$$\rho^{(p)} \ddot{\mathbf{u}}^{(p)}(\mathbf{X}, t) = \mathbf{f}_{int}^{(p)}(\mathbf{X}, t) + \mathbf{f}_{ext}^{(p)}(\mathbf{X}, t), \quad \forall (\mathbf{X}, t) \in \Omega_0^{(p)} \times (0, t_F], \quad (1)$$

⁶⁶ where $\rho^{(p)}$, $\mathbf{f}_{int}^{(p)}$, and $\mathbf{f}_{ext}^{(p)}$ are density, and internal and external force densities. The
⁶⁷ above equation is complemented with initial conditions, $\mathbf{u}^{(p)}(\mathbf{X}, 0) = \mathbf{u}_0^{(p)}(\mathbf{X})$, $\dot{\mathbf{u}}^{(p)}(\mathbf{X}, 0) =$
⁶⁸ $\dot{\mathbf{u}}_0^{(p)}(\mathbf{X})$, $\mathbf{X} \in \Omega_0^{(p)}$.

69 Internal force - State-based peridynamics

70 The internal force term $f_{int}^{(p)}(\mathbf{X}, t)$ in the momentum balance governs intra-particle deformation
71 and fracture. In PeriDEM, this term is modeled using a simplified state-based peridynamics formu-
72 lation that accounts for nonlocal interactions over a finite horizon. The specific constitutive
73 structure used—including damage-driven bond weakening, volumetric strain contributions, and
74 neighbor-weighted quadrature—is discussed in detail in (Jha et al., 2021, sec. 2.1 and 2.3).
75 This formulation allows unified simulation of deformation and fracture in individual particles.

76 DEM-inspired contact forces

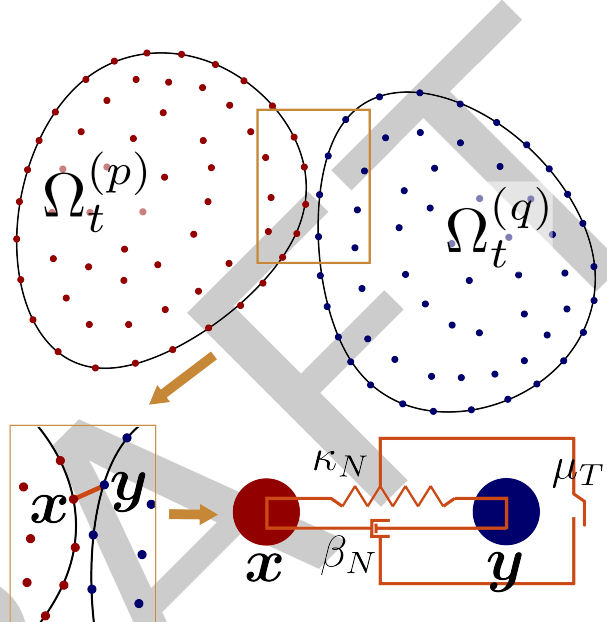


Figure 2: High-resolution contact approach in PeriDEM model for granular materials? between arbitrarily-shaped particles. The spring-dashpot-slider system shows the normal contact (spring), normal damping (dashpot), and tangential friction (slider) forces between points x and y .

77 The external force term $f_{ext}^{(p)}(\mathbf{X}, t)$ includes body forces, wall-particle interactions, and contact
78 forces from other particles. Contact is modeled using a spring-dashpot-slider formulation applied
79 locally when particles come within a critical distance. This approach introduces nonlinear normal
80 forces, damping, and friction without relying on particle convexity or simplified geometries.
81 Figure 2 illustrates the local high-resolution contact approach between deformable particles.
82 The full formulation of contact detection, force assembly, and its implementation is provided
83 in (Jha et al., 2021, sec. 2.2).

84 Implementation

85 PeriDEM is implemented in C++ and hosted on GitHub. It depends on a minimal set of
86 external libraries, most of which are bundled in the external directory. Some of the key
87 dependencies include Taskflow (Huang et al., 2021) for multithreaded parallelism, nanoflann
88 (Blanco & Rai, 2014) for efficient neighborhood search, and VTK for output and post-processing.
89 The numerical strategies for neighbor search, peridynamic integration, damage evaluation,
90 and time stepping follow those introduced in (Jha et al., 2021, sec. 3), where additional
91 implementation details and validation are discussed. The core simulation model is implemented
92 in `src/model/dem`, with the class `DEMModel` managing particle states, force calculations, and
93 time integration.

94 This work builds on earlier research in the analysis and numerical methods for peridynamics;
 95 see ([Jha & Lipton, 2018a, 2018b, 2019](#); [Jha & Lipton, 2020](#); [Lipton et al., 2019](#)).

96 Features

- 97 ▪ Hybrid modeling using peridynamics and DEM for intra-particle and inter-particle
 98 interactions
- 99
- 100 ▪ Simulation of deformation and breakage of a single particle under complex boundary
 101 conditions
- 102
- 103 ▪ Support for arbitrarily shaped particles, allowing for realistic simulation scenarios
- 104
- 105 ▪ Ongoing integration of MPI for distributed computing
- 106
- 107 ▪ Planned development of adaptive modeling strategies to enhance efficiency without
 108 compromising accuracy

109 Examples

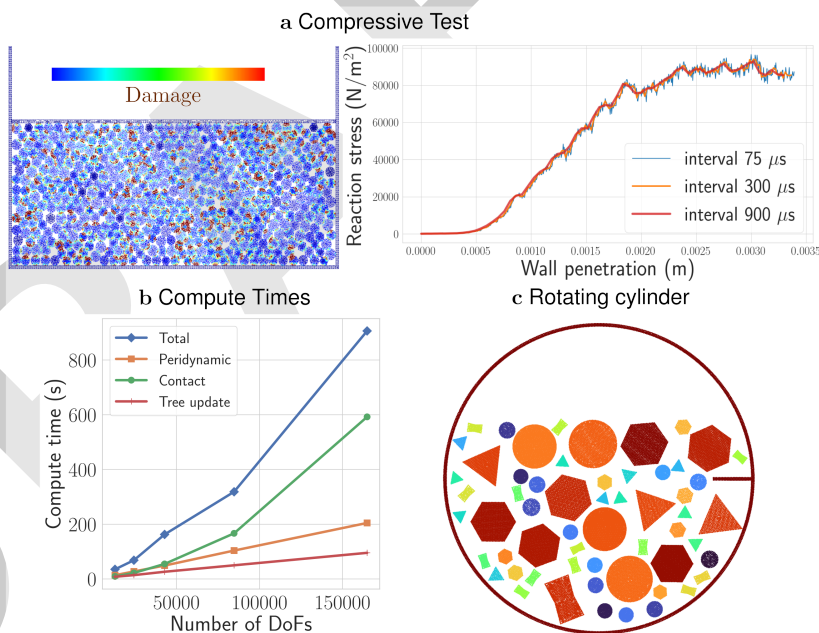


Figure 3: (a) Nonlinear response under compression, (b) exponential growth of compute time due to nonlocality of internal and contact forces, and (c) rotating cylinder with nonspherical particles.

110 Examples are described in [examples/README.md](#). One key case demonstrates compression
 111 of 500+ circular and hexagonal particles in a rectangular container by moving the top wall.
 112 The stress on the wall as a function of penetration becomes increasingly nonlinear as damage
 113 accumulates and the medium yields; see [Figure 3a](#). Preliminary performance tests show an
 114 exponential increase in compute time with the number of particles, due to the nonlocal nature of
 115 both peridynamic and contact forces, highlighting a computational bottleneck. This motivates
 116 the integration of MPI and the development of a multi-fidelity framework. Additional examples
 117 include attrition of non-circular particles in a rotating cylinder ([Figure 3c](#)).

118 Acknowledgements

119 This work was supported by the U.S. National Science Foundation through the Engineering
120 Research Initiation (ERI) program under Grant No. 2502279. The support has contributed to
121 the continued development and enhancement of the PeriDEM library.

122 References

- 123 Blanco, J. L., & Rai, P. K. (2014). *Nanoflann: A C++ header-only fork of FLANN, a library*
124 *for nearest neighbor (NN) with KD-trees.* <https://github.com/jlblancoc/nanoflann>.
- 125 Chen, Q., Li, Z., Dai, Z., Wang, X., Zhang, C., & Zhang, X. (2023). Mechanical behavior and
126 particle crushing of irregular granular material under high pressure using discrete element
127 method. *Scientific Reports*, 13(1), 7843.
- 128 Dosta, M., André, D., Angelidakis, V., Caulk, R. A., Celigueta, M. A., Chareyre, B., Dietiker, J.-
129 F., Girardot, J., Govender, N., Hubert, C., & others. (2024). Comparing open-source DEM
130 frameworks for simulations of common bulk processes. *Computer Physics Communications*,
131 296, 109066.
- 132 Govender, N., Wilke, D. N., & Kok, S. (2016). Blaze-DEMGPU: Modular high performance
133 DEM framework for the GPU architecture. *SoftwareX*, 5, 62–66.
- 134 Harmon, J. M., Karapiperis, K., Li, L., Moreland, S., & Andrade, J. E. (2021). Modeling
135 connected granular media: Particle bonding within the level set discrete element method.
136 *Computer Methods in Applied Mechanics and Engineering*, 373, 113486.
- 137 Huang, T.-W., Lin, D.-L., Lin, C.-X., & Lin, Y. (2021). Taskflow: A lightweight parallel and
138 heterogeneous task graph computing system. *IEEE Transactions on Parallel and Distributed*
139 *Systems*, 33(6), 1303–1320. <https://doi.org/10.1109/TPDS.2021.3104255>
- 140 Jha, P. K., Desai, P. S., Bhattacharya, D., & Lipton, R. (2021). Peridynamics-based discrete
141 element method (PeriDEM) model of granular systems involving breakage of arbitrarily
142 shaped particles. *Journal of the Mechanics and Physics of Solids*, 151, 104376. <https://doi.org/10.1016/j.jmps.2021.104376>
- 144 Jha, P. K., & Diehl, P. (2021). NLMech: Implementation of finite difference/meshfree
145 discretization of nonlocal fracture models. *Journal of Open Source Software*, 6(65), 3020.
146 <https://doi.org/10.21105/joss.03020>
- 147 Jha, P. K., & Lipton, R. (2018a). Numerical analysis of nonlocal fracture models in holder
148 space. *SIAM Journal on Numerical Analysis*, 56(2), 906–941. <https://doi.org/10.1137/17M1112236>
- 150 Jha, P. K., & Lipton, R. (2018b). Numerical convergence of nonlinear nonlocal continuum
151 models to local elastodynamics. *International Journal for Numerical Methods in Engineering*,
152 114(13), 1389–1410. <https://doi.org/10.1002/nme.5791>
- 153 Jha, P. K., & Lipton, R. (2019). Numerical convergence of finite difference approximations for
154 state based peridynamic fracture models. *Computer Methods in Applied Mechanics and*
155 *Engineering*, 351, 184–225. <https://doi.org/10.1016/j.cma.2019.03.024>
- 156 Jha, P. K., & Lipton, R. P. (2020). Kinetic relations and local energy balance for LEFM from
157 a nonlocal peridynamic model. *International Journal of Fracture*. <https://doi.org/10.1007/s10704-020-00480-0>
- 159 Lipton, R. P., Lehoucq, R. B., & Jha, P. K. (2019). Complex fracture nucleation and evolution
160 with nonlocal elastodynamics. *Journal of Peridynamics and Nonlocal Modeling*, 1(2),
161 122–130. <https://doi.org/10.1007/s42102-019-00010-0>

- 162 Littlewood, D. J., Parks, M. L., Foster, J. T., Mitchell, J. A., & Diehl, P. (2024). The
163 peridigm meshfree peridynamics code. *Journal of Peridynamics and Nonlocal Modeling*,
164 6(1), 118–148.
- 165 Smilauer, V., Angelidakis, V., Catalano, E., Caulk, R., Chareyre, B., Chèvremont, W., Doro-
166 feenko, S., Duriez, J., Dyck, N., Elias, J., Er, B., Eulitz, A., Gladky, A., Guo, N., Jakob, C.,
167 Kneib, F., Kozicki, J., Marzougui, D., Maurin, R., ... Yuan, C. (2021). Yade documentation
168 (3rd edition). *Zenodo*. <https://doi.org/10.5281/zenodo.5705394>
- 169 Thompson, A. P., Aktulgah, H. M., Berger, R., Bolintineanu, D. S., Brown, W. M., Crozier, P.
170 S., in 't Veld, P. J., Kohlmeyer, A., Moore, S. G., Nguyen, T. D., Shan, R., Stevens, M. J.,
171 Tranchida, J., Trott, C., & Plimpton, S. J. (2022). LAMMPS - a flexible simulation tool for
172 particle-based materials modeling at the atomic, meso, and continuum scales. *Computer
173 Physics Communications*, 271, 108171. <https://doi.org/https://doi.org/10.1016/j.cpc.2021.108171>
- 175 Zhang, R., Tagliafierro, B., Vanden Heuvel, C., Sabarwal, S., Bakke, L., Yue, Y., Wei, X.,
176 Serban, R., & Negrut, D. (2024). Chrono DEM-Engine: A discrete element method
177 dual-GPU simulator with customizable contact forces and element shape. *Computer
178 Physics Communications*, 300, 109196. <https://doi.org/https://doi.org/10.1016/j.cpc.2024.109196>